

# Research Journal of Pharmaceutical, Biological and Chemical Sciences

## Simulation Of Flow Separation At The Inlet Of A Projecting Flat Suction Channel

Olga A. Averkova\*, Ilya V. Kryukov, Kirill V. Plotnikov, Elena I. Tolmacheva, and Ilya V. Khodakov.

Belgorod State Technological University Named After V.G. Shoukhov, Kostyikova Str., 46, Belgorod 308012, Russia.

### ABSTRACT

The task of separated flow slit-shaped suction flue is solved with the help of usage the theory of functions of a complex variable and stromfadentheorie. Velocity diagram was formulated and streamline configuration was found. The received calculation results are compared with discrete vortex method, root-finding algorithm, Reynolds-averaged Navier-Stokes, equation of continuity and experimental data. Then the conclusion about conformity and authenticity of received design quantity and velocity diagram is made up. The studies will be useful for specialists in the field of industrial ventilation and aerodynamics of separated flows. This study focuses on the numerical and experimental study of a separated flow at the inlet of a slot-type hooded suction inlet. Thus, the model of potential separated flows adequately describes most of the real suction flare of a flat slot. The behavior of the relative velocity of the jet separation is almost identical to the experimental law of change in the local drag coefficient depending on the length of the projections adjacent to the inlet. Horizontal shield length equal to half the width of the suction channel enables to reduce the flow of air entering into the suction channel due to effect separation of the jet.

**Keywords:** Ideal Incompressible Fluid Flow Theory, Zhukovskii Method, Local Drag Coefficient

*\*Corresponding author*

**INTRODUCTION**

The use of analytic functions theory has fruitfully effected on plane potential flows researches, especially in conformal reflections. The authors of the article were attracted by the classical problems of motion of the suction air flow in slotted holes both early and later works [1,2,3,4]. Intense interest in aerodynamics is appeared not only in practical value for applied problems of industrial ventilation [5,6,7,8] but also in dissatisfaction about the fact that in most cases, only simple mathematical models of are used in practical application. They give us quite good results in remote fields of suction jet.

We consider that there is a little number of works devoted to research of the flows close to suction hole especially practical investigations and comparison their results with the theoretical ones.

We think that it explains the lack of interest of practical men to the results of numerous researches of theoretical models.

**MATERIALS AND METHODS**

Assume that an infinitely wide horizontal pipe with a width 2B is projected to a distance S from the vertical wall. The pipe axis is directed along the axis OX of the physical plane of the complex variable  $z = x+iy$ . We will consider the upper part of the flow in the semi-plane  $y \geq 0$ . We will use the upper semi-plane of the complex variable  $t = x_1+iy_1$  as a parametric one. The correspondence of the points in these ranges, as well as the ranges of the unknown quantities of the Joukowski function  $\omega = \ln \frac{u_\infty}{u} + i\theta$  and the complex potential function  $w = \varphi+i\Psi$ , are shown in **Fig. 1**.

Here,  $u_\infty$  is the velocity value on the "free" flow line CD,  $u$  is also in the arbitrary points of the area under review in the quadrilateral ADCBA of the physical area  $\text{Im}(z) \geq 0$ . The quadrilateral has two vertexes at infinity: the point A, at which a line source with a strength  $q$  is placed and the point D, where a sink with the same strength is placed.

Thus, the range of the complex potential is a band bounded by the flow lines  $\Psi = 0, \Psi = q$  and equipotential lines at infinity  $\varphi = \pm\infty$  and the range of the Joukowski function is a half-band with a cut along the ray MA( $\theta = -\pi/2$ ) bounded by horizontal lines  $\theta = 0$  and  $\theta = -\pi$  ( $\theta$  is the angle between the positive axis OX and the direction of the velocity vector  $\vec{u}$ ).

Find a conformal mapping of the upper semi-plane  $\text{Im}(t) > 0$  onto the interior of the range  $\omega$  (the interior of the pentagon ADCBMA with two vertexes at infinity). We use the Schwarz-Christoffel integral, after simple transformations taking into account the transition conditions of the singular points B and B on semicircles  $t = b + \varepsilon_b e^{i\alpha}$  and  $t = 1 + \varepsilon_a e^{i\alpha}$  ( $\varepsilon_b \rightarrow 0, \varepsilon_a \rightarrow 0, \alpha = \pi \cdot 0$ ), as well, taking into account the correspondence of the points C and M, we find the desired Joukowski function:

$$\omega = \frac{1}{2} \ln \left( \frac{\sqrt{t} + \sqrt{b}}{\sqrt{t} - \sqrt{b}} \times \frac{\sqrt{t+1}}{\sqrt{t-1}} \right) = \ln \frac{\sqrt{t} + \sqrt{b}}{\sqrt{t-b}} \times \frac{\sqrt{t+1}}{\sqrt{t-1}} \tag{1}$$

And define the parameter:

$$\mu = \ln \frac{1+b^{1/4}}{1-b^{1/4}} \tag{2}$$

Using the same techniques, find the complex potential function:

$$w = \frac{q}{\pi} \ln(t-1) \tag{3}$$

Describing the velocity field in the semi-plane  $\text{Im}(t) > 0$  that is induced by a line source at the point A.

Bearing in mind that:

$$z = \frac{1}{u_\infty} \int_{t_k}^t e^{\omega(t)} \cdot \frac{dw}{dt} dt + z_k \quad (4)$$

And:

$$v = \frac{dw}{dz} = u_\infty e^{-\omega(t)} \quad (5)$$

And if we use the functions found  $\omega$  and  $w$  and take as a reference point  $C(t_k = 0; z_k = B.i)$ , we obtain a parametric solution of the problem:

$$z = \frac{\delta_\infty}{\pi} \int_0^T \frac{\sqrt{t+\sqrt{b}}}{\sqrt{t-b}} \cdot \frac{\sqrt{t+1}}{(t-1)^{3/2}} dt + i \quad (6)$$

$$v \equiv u_x - iu_y = \frac{\sqrt{T-b}}{\sqrt{T+\sqrt{b}}} \cdot \frac{\sqrt{T-1}}{\sqrt{T+1}} \quad (7)$$

Enabling to build a hydrodynamic grid ( $\Psi = 0.1 = \text{const}$ ;  $\varphi = -\infty..+\infty = \text{const}$ ) and the velocity field:

$$u_x = \text{Re}(v); u_y = -\text{Im}(v) \quad (8)$$

Hereinafter, the linear dimensions are related to the half-height of the slot  $B$  and the velocities to the velocity  $u_\infty$ ;  $\delta_\infty$  is the dimensionless half-height of the jet for  $t \rightarrow \infty$  (at the point  $D$ ),  $T = m+n.i$  is an arbitrary point of the upper semi-plane  $\text{Im}(t) > 0$  and a point of physical half-plane  $\text{Im}(z) > 0$  corresponding to it owing to (6), in which we define the velocity vector projection  $\vec{u}$ .

The maximum speed equal to (9) (due to the fact that at this point  $T \equiv \sqrt{b}$ ,  $b = 0.1$ ) is seen at the point  $M$  on the ray  $BA$ :

$$u_M = u_y = -\frac{1-b^{1/4}}{1+b^{1/4}} \quad (9)$$

It is easy to determine the position of this point in the physical plane:

$$x_M = S = \frac{\delta_\infty}{\pi} \int_0^{b-\varepsilon} \frac{\sqrt{t+\sqrt{b}}}{\sqrt{b-t}} \cdot \frac{1+\sqrt{t}}{(1-t)^{3/2}} dt \quad (10)$$

$$y_M = 1 + \frac{\delta_\infty}{\pi} \int_{b+\varepsilon}^{\sqrt{b}} \frac{\sqrt{t+\sqrt{b}}}{\sqrt{b-t}} \cdot \frac{1+\sqrt{t}}{(1-t)^{3/2}} dt, \quad \varepsilon \rightarrow 0 \quad (11)$$

We find the coordinates of the flow line  $CD$  to determine the half-height of the jet at infinity  $\delta_\infty$ .

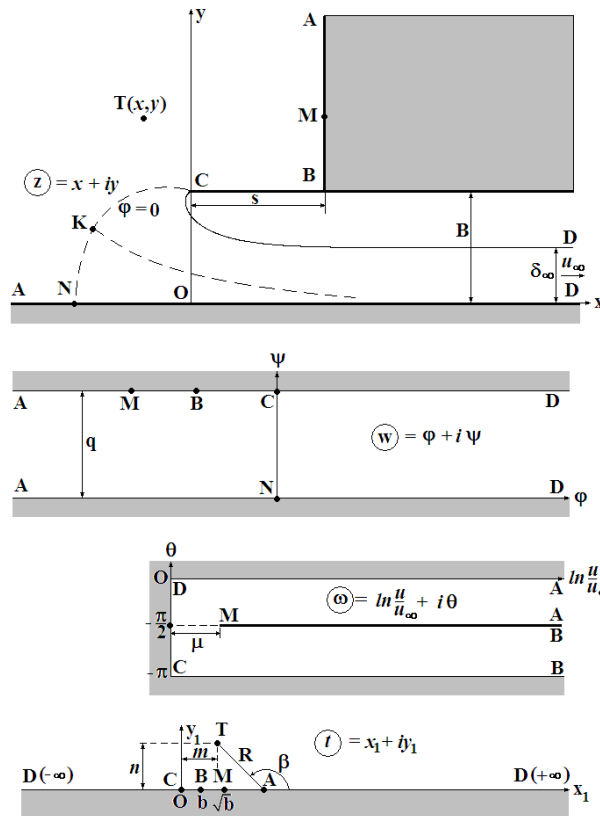


Fig.1. To the determination of the separated flow near a projecting suction slot

Given that the points of this line correspond to the points on the negative semi-axis  $OX_1$  ( $-\infty < t < 0$ ) based on (6) we can write the following system of equations:

$$x_{CD} = \frac{\delta_\infty}{\pi} \int_0^\eta \frac{(v - \sqrt{b}) dv}{\sqrt{b+v}(1+v)^{1.5}} \quad (12)$$

$$y_{CD} = 1 - (1 + \sqrt{b}) \frac{\delta_\infty}{\pi} \int_0^\eta \frac{\sqrt{v} dv}{\sqrt{b+v}(1+v)^{1.5}}, \quad 0 \leq \eta < +\infty, \quad (13)$$

Describing the coordinates of the line CD in the upper semi-plane of the physical space. Given that  $y_{DC} \rightarrow \delta_\infty$  for  $\eta \rightarrow \infty$ , we have  $\delta_\infty = 1 - \frac{\delta_\infty}{\pi} E(b)$  whence it follows:

$$\delta_\infty = \pi / (\pi + E(b)) \quad (14)$$

where,  $E(b)$  is the number depending on the parameter  $b$ :

$$E(b) = (1 + \sqrt{b}) \int_0^\infty \frac{\sqrt{v} dv}{\sqrt{b+v}(1+v)^{1.5}} \quad (15)$$

Taking into account the result obtained based on (10) we can write the following relationship:

$$S = \frac{1}{\pi + E(b)} \int_0^{b-s} \frac{\sqrt{t + \sqrt{b}}}{\sqrt{b-t}} \cdot \frac{1 + \sqrt{t}}{(1-t)^{1.5}} dt \quad (16)$$

Connecting the length of the projection (hood) with the parameter  $b$ . In particular, for  $b = 0$  we have:

$$E(0) = \int_0^{\infty} \frac{dv}{(1+v)^{1.5}} = 2; \delta_{\infty} = \frac{\pi}{\pi+2}; S = 0; \mu = 0 \tag{17}$$

i.e., the case of a separated air flow at the slot-type suction built into a flat unlimited wall. In this case, the relations to determine the velocity field as well as the coordinates of the free flow line *CD* are much simplified:

$$x + y \cdot i = \frac{1}{\pi+2} \int_0^t \frac{\sqrt{t+1}}{(t-1)^{1.5}} dt + i = \frac{2}{\pi+2} \left[ \ln(\sqrt{T-1} + \sqrt{T}) - \frac{1+\sqrt{T}}{\sqrt{T-1}} \right] \tag{18}$$

$$u_x - iu_y = \frac{\pi+2}{\pi} \cdot \frac{\sqrt{T-1}}{\sqrt{T+1}} \tag{19}$$

$$x_{CD} = \frac{2}{\pi+2} \left[ \ln(\sqrt{\eta+1} + \sqrt{\eta}) - \frac{\sqrt{\eta}}{\sqrt{\eta+1}} \right] \tag{20}$$

$$y_{CD} = \frac{2}{\pi+2} \left[ \frac{\pi}{2} + \frac{1}{\sqrt{\eta+1}} \right]; \eta = 0..{\infty} \tag{21}$$

For *b* = 1, we have another classic case of the separated air flow at the slot-type suction in infinite space:

$$E(1) = 2 \int_0^{\infty} \frac{\sqrt{v}}{(1+v)^2} dv = \pi, \quad \delta_{\infty} = 0.5 \tag{22}$$

$$S = \frac{1}{2\pi} \int_0^1 \frac{\sqrt{t+1}}{(1-t)^2} dt \rightarrow \infty, \quad \mu \rightarrow \infty$$

**Table 1. Main parameters of the separated flow at a projecting suction slot**

<i>b</i>	<i>E(b)</i>	<i>S(b)</i>	$\delta_{\infty}(b)$	<i>W(b)</i>	$\mu(b)$	$\mu_M$	<i>Y<sub>M</sub></i>
0.00	2.000	0.0000	0.6110	1.637	0.0000	-1.00000	1.000
0.02	2.240	0.0151	0.5838	1.713	0.4717	-0.45340	1.068
0.04	2.325	0.0317	0.5747	1.740	0.5928	-0.38200	1.112
0.06	2.386	0.0496	0.5684	1.759	0.6830.0000	-0.33790	1.153
0.08	2.435	0.0689	0.5633	1.775	0.7589	-0.30560	1.193
0.10	2.477	0.0894	0.5591	1.789	0.8263	-0.28010	1.232
0.12	2.514	0.1114	0.5555	1.800	0.8881	-0.25900	1.272
0.14	2.547	0.1348	0.5522	1.811	0.9460	-0.24090	1.313
0.16	2.577	0.1597	0.5493	1.820	1.0010	-0.22510	1.354
0.18	2.605	0.1863	0.5467	1.829	1.0540	-0.21110	1.397
0.20	2.630	0.2146	0.5443	1.837	1.1050	-0.19850	1.441
0.22	2.654	0.2448	0.5420	1.845	1.1550	-0.18700	1.486
0.24	2.677	0.2770	0.5399	1.852	1.2040	-0.17650	1.534
0.26	2.698	0.3114	0.5380	1.859	1.2520	-0.16680	1.583
0.28	2.718	0.3481	0.5361	1.865	1.3000	-0.15780	1.635
0.30	2.738	0.3874	0.5344	1.871	1.3470	-0.14940	1.689
0.32	2.756	0.4294	0.5327	1.877	1.3950	-0.14150	1.746
0.34	2.773	0.4744	0.5311	1.883	1.4420	-0.13400	1.806
0.36	2.790	0.5228	0.5296	1.888	1.4900	-0.12700	1.870
0.38	2.806	0.5747	0.5282	1.893	1.5380	-0.12040	1.937
0.40	2.822	0.6307	0.5268	1.898	1.5860	-0.11400	2.008
0.42	2.837	0.6910	0.5255	1.903	1.6350	-0.10800	2.084

0.44	2.852	0.7562	0.5242	1.908	1.6840	-0.10230	2.165
0.46	2.866	0.8269	0.5230	1.912	1.7350	-0.09676	2.252
0.48	2.879	0.9036	0.5218	1.917	1.7860	-0.09149	2.345
0.50	2.893	0.9872	0.5206	1.921	1.8380	-0.08643	2.446
0.52	2.905	1.0780	0.5195	1.925	1.8920	-0.08156	2.554
0.54	2.918	1.1780	0.5185	1.929	1.9470	-0.07687	2.672
0.56	2.930	1.2880	0.5174	1.933	2.0030	-0.07235	2.800
0.58	2.942	1.4090	0.5164	1.936	2.0610	-0.06799	2.940
0.60	2.954	1.5440	0.5154	1.940	2.1210	-0.06377	3.093
0.62	2.965	1.6930	0.5145	1.944	2.1840	-0.05968	3.263
0.64	2.976	1.8600	0.5135	1.947	2.2480	-0.05573	3.451
0.66	2.987	2.0480	0.5126	1.951	2.3160	-0.05189	3.661
0.70	3.008	2.5040	0.5109	1.957	2.4610	-0.04455	4.164
0.74	3.028	3.1080	0.5092	1.964	2.6240	-0.03762	4.820
0.76	3.037	3.4890	0.5084	1.967	2.7130	-0.03429	5.230
0.80	3.056	4.4890	0.5069	1.973	2.9140	-0.02789	6.294
0.84	3.075	6.0080	0.5054	1.979	3.1550	-0.02179	7.888
0.88	3.092	8.5630	0.5040				
1.984							
	3.4590	-0.01598	10.54				

$$x + y \cdot i = \frac{1}{\pi} \left[ \ln(\sqrt{T} - 1) - \frac{\sqrt{T}}{\sqrt{T} - 1} \right] \quad (23)$$

$$u_x - iu_y = \frac{1}{2} \cdot \frac{\sqrt{T} - 1}{\sqrt{T} + 1} \quad (24)$$

$$x_{CD} = \frac{1}{\pi} \left( \ln \sqrt{1 + \eta} - \frac{\eta}{\eta + 1} \right) \quad (25)$$

$$y_{CD} = \frac{1}{\pi} \left( \pi - \arctg \sqrt{\eta} + \frac{\sqrt{\eta}}{\eta + 1} \right), \quad \eta = 0.. \infty \quad (26)$$

For the general case of (b = 0..1; S = 0..∞) based on the numerical solution of equations (15), (16), (11) and calculations by (2), (9), (14), the parameters of the problem are given in **Table 1**.

There can be some difficulties in constructing a hydrodynamic grid (a family of orthogonal curves φ = const; Ψ = const) and determining the velocity field that are related to finding the integral (6) which is not expressed in terms of elementary functions (it can only be reduced to the sum of elliptic integrals).

In this case, we can use numerical methods, assuming that the constants δ∞ and b are known for a given S (for example, they can be taken from **Table 1** or from the solution of (16) and δ∞ can be calculated by the formula (14).

After the integrand is divided by the real and imaginary parts, the integral (6) is reduced to a sum of contour integrals. In this case, we use the analytic property of the integrand enabling the arbitrary choice of the integration path between the points C(0, 0) and T(m; n). The best option is to integrate first in a circumferential direction (centered at t = 1) with a radius r = 1 from the point C to the intersection with the ray AT and then along this ray from the intersection point to the preset point T.

### RESULTS

Four vertical sections of the jet in the suction slot (located at x/B = 0.05; 0.3; 0.55 and 0.8 from the input section, respectively) and three horizontal sections were selected as typical sections: under (y/B = 0.8), at a level (y/B = 1) of and above (y/B = 1.2) the hood. With a measurement pitch of 0.1B, the horizontal component of the velocity vector u<sub>x</sub> was measured in the first case and the vertical one u<sub>y</sub> in the second case. The results are shown in Fig. 2 and 3. Here the solid lines show the calculation results in Maple-9 using (6) and (7) for S/B = 1,0 (b = 0.50286, δ∞ = 0.520474).

For comparison we also show the velocity profiles obtained by the Discrete Vortex Methods (DVM) and by solving the time-averaged Reynolds-Averaged Navier-Stokes equation (RANS) in the Fluent software. As can be seen from these results, the theoretical description of the velocity field with models of separated flows presents a practically sufficiently accurate description of the behavior of the velocity components, except for the areas near the jet separation and on its free boundary (*CD*). Here, we have a fully developed turbulence; and due to this, the potentiality of the flow seems to be violated. For example, in the vertical sections of the channel near the line *CD* (Fig. 2), a well-pronounced boundary mixing layer is seen with a sharp change in the horizontal component of velocity and a significant deviation of the experimental values from the theoretical ones with an increase in the distance of the metering sections from the air inlet into the channel. The theoretical value  $u_x$  exceeds the empirical one due to the fact that the true thickness is higher than the theoretical one  $\delta$ . The dead zone (between *CB* and *CD*) is filled with a moving stream, although its velocities are low. Naturally, the velocity within the theoretical jet separation will be lower in this case.

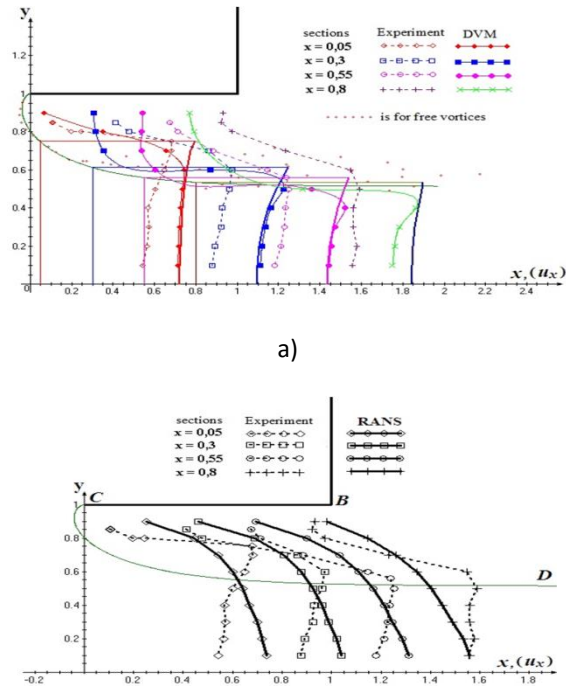


Fig.2. Measurement of the longitudinal air velocity through the entire height of the flat channel equipped with a hood of a unit length

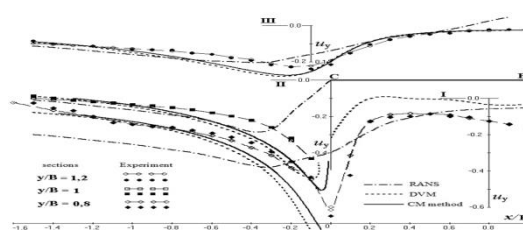


Fig.3. Change in the vertical velocity component near the inlet of the hooded suction slot (*CB*) of unit length; on the orthographic representations, solid lines are theoretical values; circles, diamonds, squares are experimental values; I,II,III are the velocity profiles in the cross sections  $y/B = 0.8; 1; 1.2$ , respectively)

As to the qualitative description, the experimental data are in good agreement with the theoretical values. The longitudinal velocities increase in each section towards the boundary *CD*, the peak area (similar to the line *CD*) becomes more distant from the hood. The dead zone is filled with a flow whose velocity is significantly lower than the velocity within the range of the jet (between the lines *CD* and *AD*).

In horizontal sections, the greatest deviation from the theoretical values is also observed near the separation point, although the qualitative character of the change in the vertical component of velocity is in good agreement with the experimental values: the highest value  $u_y$  both in the experimental studies and the

theoretical ones by the CM method and DVM [2,3,9,10,11,12] is seen near the point C (Fig. 3). The more distant it is from the point C, the closer the value of the measured  $u_y$  is to the theoretically calculated one. At a distance 0.5..0.8B, the deviations will not interrupt the measurement errors. Note that the RANS method gives values close to 0 in the range C.

Thus, the model of potential separated flows can be deemed to adequately describe the nature of the flows almost in the whole area of the suction flare. Some convention in the existence of a “break” of flows on the free boundary CD does not prevent the widespread use of jet contraction (namely  $\delta_\infty$ ) in practical determination of the pressure losses. The main cause of energy losses during the inlet into the inlets is undoubtedly the gating effect of the flow which is separated from the walls adjacent to this inlet. The longer is the length of these walls (hoods, projections), the greater is the separation velocity the higher is the strength of the flow flowing to the inlet and, consequently, the higher are pressure losses.

**DISCUSSION**

We show this by two specific examples: air inlet into a flat pipe and its outflow from a flat pipe through the diaphragm. These examples have been chosen due to the availability of the experimental data obtained by [13].

We will use the difference in velocities on a free surface (separation velocity) and the average velocity in the slotted opening to describe the value of inertia:

$$\Delta u = \frac{u_\infty^* - u_{in}^*}{u_{in}^*} \equiv w(b) - 1; w(b) = \frac{u_\infty^*}{u_{in}^*} = \frac{1}{\delta_\infty(b)}$$

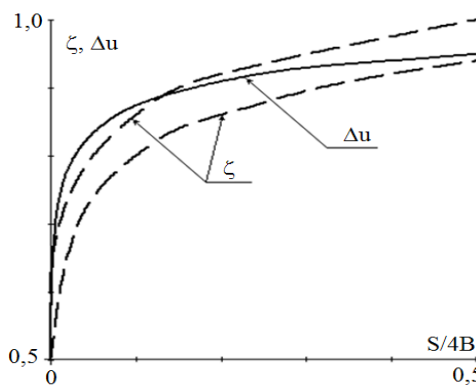


Fig.4. Change in the local drag coefficient at the inlet into the flat pipe ( $\zeta$ ) and the jet separation velocity ( $\Delta u$ ) with increasing in the projection length ( $S/4B$ ): The solid line is based on theoretical data (Table 1), dashed ones on experimental data by I.E. Idelchik (Curve 1 for the relative wall thickness of, Curve 2 for  $\delta/D_F = 0.004$ )

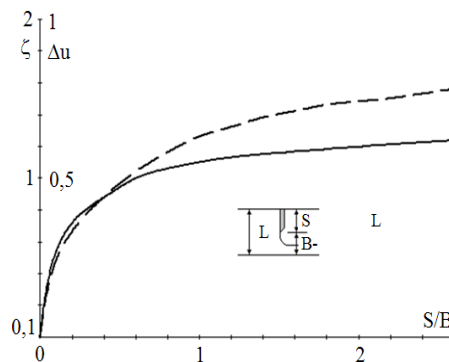


Fig.5. Change in the local drag coefficient at the inlet into the flat pipe ( $\zeta$ ) and the jet separation velocity ( $\Delta u$ ) with increasing in the projection length ( $S/B$ ): The solid curve based on equations (27) and (28), the dotted one represents the experimental data by I.E. Idelchik

We use the data from **Table 1** to determine the theoretical coefficient of jet contraction  $\delta_\infty = \delta_\infty^* / B^*$  (the values  $\delta_\infty^*$ ,  $B^*$  are dimensional, which is shown by the superscript \*) for an inlet into a flat pipe; and we use the results of theoretical studies by Zhukovsky and R. von Mises described in [14,15] to assess the degree of flow contraction in the outflow through the diaphragm:

$$\delta_\infty \equiv \frac{\delta_\infty^*}{B^*} = \frac{\pi}{\pi + 2 \frac{2\alpha}{\text{tg}2\alpha}}; n \equiv \frac{B^*}{L^*} = \frac{\text{tg}\alpha}{\delta_\infty}$$

Whence:

$$S \equiv S^* / B^* = 1 / n - 1 = \delta_\infty / \text{tg}\alpha - 1$$

where,  $\alpha$  is the parameter varying within  $0 \leq \alpha \leq \pi/4$ . The latter can be eliminated, allowing for a direct connection between  $\delta_\infty$  and  $n$  (or  $S$ ) in the form of a transcendental equation:

$$\delta_\infty = \pi / (\pi + 2 \cdot A) \tag{27}$$

where,  $A = A_n$  is the function of  $\delta_\infty$  and  $n$ :

$$A_n = (1 / n\delta_\infty - n\delta_\infty) \text{arctg}(n\delta_\infty)$$

or of  $\delta_\infty$  and  $S$ :

$$A = A_S = \left( \frac{S+1}{\delta_\infty} - \frac{\delta_\infty}{S+1} \right) \text{arctg} \left( \frac{\delta_\infty}{S+1} \right) \tag{28}$$

It is easy to see that for  $S = 0$  ( $n = 1$ ), the coefficient of contraction is  $\delta_\infty = 1$  (no contraction occurs) and for  $S \rightarrow \infty$  ( $n = 0$ ) the function  $A = 1$ ,  $\delta_\infty = 0.611$  (the outflow through holes in an infinite wall).

As can be seen from **Fig. 4 and 5**, the relative separation velocity  $\Delta u$  is increasing with an increase in the length of a straight wall before the outflow of the jet; and the nature of this increase corresponds with the change in the local drag coefficient.

### CONCLUSION

Thus, the model of potential separated flows adequately describes most of the real suction flare of a flat slot. Significant deviations of the theoretical velocity field from the experimental one are only seen in the jet separation area and on its free boundary. A developed boundary layer with a great transverse gradient of the longitudinal velocities is seen along the free boundary of the jet in the channel.

The degree of the cross section jet contraction in a channel is determined by the inertia of the airflow flowing along flat surfaces at the inlet into the suction slot. The bigger is the acceleration path of this flow, the higher is the rate of its separation and the more pronounced is the gating effect at the air inlet into the inlet. The behavior of the relative velocity of the jet separation is almost identical to the experimental law of change in the local drag coefficient depending on the length of the projections adjacent to the inlet.

Note that in this study used the methods of the theory of functions of a complex variable. Using such methods ensures the most accurate results. There is an analytical solution obtained in some of the simplest cases. The problem often resolves oneself into quite lengthy non-linear equations with coefficients of unknown variables in the form of Cauchy type integrals. In the general case when a multiply connected flow region or, all the more, a three-dimensional space is considered solving the problems using the methods above is impossible. This drawback can be removed in the future, using the method of discrete vortices. In what is supposed to use this method for the study of separated flows at the inlet to the suction channels with a few

thin visors. The results will be useful to reduce the amount of air entering the slit nondensity aspirating shelters.

#### ACKNOWLEDGEMENT

The researchers are being supported by the Council for Grants of the President of the Russian Federation (projects MK-103.2014.1), RFBR (project number 14-08-31069 mol\_a) and Strategic Development Plan of BSTU named after. V. G. Shukhov.

#### REFERENCES

- [1] O. A. Averkova, V.U. Zorya, I.N. Logachev and K.I. Logachev, "Numerical simulation of air currents at the inlet to slot leaks of ventilation covers," *Refractories Indus. Ceramics*, vol. 51, pp. 177-182, 2010. DOI: 10.1007/s11148-010-9284-7
- [2] O.A. Averkova, I. N. Logachev, K.I. Logachev, A.K. Logachev, "The principles of separated flow at the inlet of the protruding duct with screens," *TsAGI Sci. J.*, vol. 44, pp. 219-243, 2013. URL: <http://www.dl.begellhouse.com/journals/58618e1439159b1f,5cadfcb91b5f9b0f,44a9ff1d2cc6fb75.html>
- [3] O.A. Averkova, I.N. Logachev, K.I. Logachev and I.V. Khodakov, "About the modeling of detachable flows on the entrance of the round soaking-up branch pipe," *Middle-East Journal of Scientific Research*, vol. 17 (8), pp. 1187-1193, 2013. DOI: 10.5829/idosi.mejsr.2013.17.08.7095
- [4] O.A. Averkova, I.N. Logachev, K.I., Logachev, I.V. Khodakov, "Modeling detached flows at the inlet to round suction flues with annular screens," *Refractories Indus. Ceramics*, vol. 54, pp. 425-429, 2014. DOI: 10.1007/s11148-014-9625-z
- [5] V.A. Minko, I.N. Logachev, K.I. Logachev et al., "Dedusting ventilation", Printing Office of the V.G.Shukhov State Technology University of Belgorod, Belgorod, vol. 2, pp. 565, 2010.
- [6] R.L.Wabeke, "Air Contaminants, Ventilation, and Industrial Hygiene Economics: The Practitioner's Toolbox and Desktop Handbook". - CRC Press, Boca Raton, 2010. ISBN: 978-1466577909
- [7] I.N. Logachev, K. I. Logachev and O.A. Averkova, "Methods and means of reducing the power requirements of ventilation systems in the transfer of free-flowing materials," *Refractories Indus. Ceramics*, vol. 54, pp. 258-262, 2013. DOI: 10.1007/s11148-013-9585-8
- [8] I.N. Logachev, I.N. and K.I. Logachev, "Industrial Air Quality And Ventilation: Controlling Dust Emissions". - CRC Press, Boca Raton, 2014. ISBN:9781482222166
- [9] R. Schinzinger, P.A.A. Laura, "Conformal Mapping: Methods and Applications (Dover Books on Mathematics)". - New York: Dover Publications, 2012. ISBN:9780486150751
- [10] O.A. Averkova, A.E. Canar, K.I. Logachev, V.A. Uvarov, "Simulation of processes of ventilation in the confided area of trapezoidal form," *Middle-East Journal of Scientific Research*, vol. 17 (8), pp. 1176-1180, 2013. DOI: 10.5829/idosi.mejsr.2013.17.08.7093
- [11] O.A. Averkova, V.I. Belyaeva, K.I. Logachev, V.A. Uvarov, A.E. Canar, "About dynamics of clinker dust in an aspiration hideout," *Middle-East Journal of Scientific Research*, vol. 17 (8), pp. 1181-1186, 2013. DOI: 10.5829/idosi.mejsr.2013.17.08.7094
- [12] J.S. Marshall, Li. Shuiqing, "Adhesive Particle Flow: A Discrete-Element Approach". - Cambridge: Cambridge University Press, 2014. ISBN-13: 978-1107032071.
- [13] I.E. Idelchik, "Handbook of Hydraulic Resistance". - New York: Begell House, 2008. ISBN: 978-1-56700-251-5.
- [14] I.N. Logachev, K. I. Logachev and O. A. Averkova, "Mathematical modeling of separated flows at inlet of a shielded flat duct," *Computational methods and programming*, vol. 11(1), pp.68-77, 2010.
- [15] I.N. Logachev, K. I. Logachev, V.Yu. Zorya and O.A. Averkova, "Modeling of separated flows next to suction slots," *Computational methods and programming*, vol. (11), pp.43-52, 2010